International Journal of Pharmaceutics 406 (2011) 78–83

Contents lists available at ScienceDirect

International Journal of Pharmaceutics

journal homepage: www.elsevier.com/locate/ijpharm

A nuclear magnetic resonance approach to the comparison of mucoadhesive properties of polysaccharides for ophthalmic uses

Gloria Uccello-Barretta[a,*], Samuele Nazzi[b], Federica Balzano[a], Marco Sansò[c]

[a] Dipartimento di Chimica e Chimica Industriale, Università di Pisa, Via Risorgimento 35, I-56126 Pisa, Italy
[b] Istituto per i Processi Chimico-Fisici – CNR, Area della Ricerca, Via G. Moruzzi 1, I-56124 Pisa, Italy
[c] Farmigea S.p.A., Via G. B. Oliva 8, I-56121 Pisa, Italy

ARTICLE INFO

Article history:
Received 29 July 2010
Accepted 29 December 2010
Available online 8 January 2011

Keywords:
Nuclear magnetic resonance
Polymer interaction
Mucoadhesion
Eye-drop excipient

ABSTRACT

Mucoadhesive properties of tamarind seed polysaccharide (TSP) and larch arabinogalactan (AG), which are developed for ophthalmic applications, were investigated by NMR spectroscopy. Polysaccharide to mucin affinities were compared by using ketotifen fumarate as low molecular weight interaction probe. Proton selective relaxation rate measurements revealed enhanced affinity of TSP to mucin with respect to AG.

1. Introduction

The mucoadhesive behaviour of polymeric materials depends on their affinity to mucin and it has been the subject of numerous studies during the last 20 years. *In vivo* methods for mucoadhesion evaluation are relatively scarce, probably because they cannot discriminate between mucoadhesion and other factors affecting the residence time, and they are often accompanied by large standard deviations (Edsman and Hägerström, 2005). Several *in vitro* methods have been developed (Ch'ng et al., 1985; Ponchel et al., 1987; Smart et al., 1984; Hassan and Gallo, 1990), among which the rheological method is one of the most extensively used due to its inherent simplicity, even if the results strongly depend on experimental conditions (Hägerström and Edsman, 2003).

The relevance of the development of efficient, reproducible and quick non-invasive methods for comparing polysaccharides to mucin affinity to be correlated to their mucoadhesive properties, addressed towards the use of spectroscopic techniques (Hägerström et al., 2005). Among them, nuclear magnetic resonance (NMR) spectroscopy represents a powerful technique, as all molecules have NMR active nuclei, and due to the advantage of non-alteration of the normal bio-functionality of the biomolecules under investigation. As a matter of fact, mucin/polymer interaction processes have been investigated by ^{1}H and/or ^{13}C NMR spectroscopy (Mortazavi, 1995; Patel et al., 2003) or by NMR diffusion measurements (Griffiths et al., 2010). Recently, we demonstrated the great efficacy of proton selective relaxation rate measurements in the non-invasive evaluation of drug–polysaccharide affinities, which could give new perspectives to the rational design of new formulations for medical uses (Uccello-Barretta et al., 2008; Uccello-Barretta et al., 2010).

Among polysaccharides employed for ophthalmic uses, tamarind-seed polysaccharide (TSP) showed great potentiality in the development of artificial tears for the treatment of the dry eye disease (Rolando and Valente, 2007) or in the formulation of drugs to be employed in ophthalmic field (Ghelardi et al., 2000; Uccello-Barretta et al., 2008; Di Colo et al., 2009). A water-soluble arabinogalactan (AG), which is abundant in Western larch, and is constituted of a backbone of β-(1 → 3) linked D-galactopyranose residues (Ponder, 1998; Chandrasekaran and Janaswamy, 2002), has been also proposed as an alternative to TSP (Burgalassi et al., 2007). The mucoadhesive properties of these two vegetal macromolecules have been recently put in comparison by rheological methods (Burgalassi et al., 2007; Di Colo et al., 2009), with contradictory results.

In consideration of the potential technological relevance of such kind of polysaccharides, we exploited NMR proton selective relaxation rate methods for comparing mucoadhesive properties of TSP and AG. To this aim, we employed ketotifen fumarate (KT) as interaction probe, by detecting the effect of the presence of TSP or AG on the KT–mucin interaction. Indeed, affinity of KT to mucin has been already demonstrated (Uccello-Barretta et al., 2010) and

* Corresponding author. Tel.: +39 0502219232; fax: +39 0502219260.
E-mail address: gub@dcci.unipi.it (G. Uccello-Barretta).

0378-5173/$ – see front matter © 2011 Elsevier B.V. All rights reserved.
doi:10.1016/j.ijpharm.2010.12.032

any polysaccharide to mucin interaction is expected to perturb KT–mucin affinity.

2. Materials and methods

2.1. Materials

Bovine submaxillary mucin (BSM) and phosphate buffer powder were purchased from Sigma–Aldrich. Ketotifen fumarate (Sifavitor S.p.A, Lodi, Italy) and tamarind-seed polysaccharide, MW 700 kDa (Opocrin S.p.A., Modena, Italy) were kindly gifted by Farmigea S.p.A (Pisa, Italy). Arabinogalactan, MW 10.120 kDa (Fiberaid®) was purchased from Sochim International S.p.A. (Milan, Italy). All chemicals were used without any further purification.

2.2. Methods

All NMR samples were prepared in D_2O solution in the presence of phosphate buffer (pH 7.4) 0.1 M. Macromolecule solutions were prepared by dissolution in the solvent by stirring into vials. All samples were obtained by mixing different volumes of stock solutions of the appropriate amounts of drug and macromolecule into vials.

NMR measurements were performed on spectrometer operating at 600 MHz for ^{1}H. The temperature was controlled to $25 \pm 0.1\,^{\circ}$C. The longitudinal selective relaxation rates were measured in the initial rate approximation (Freeman and Wittekoek, 1969) by employing a selective π-pulse at the selected frequency. The π selective inversion of the proton spin population was obtained by a selective soft perturbation pulse. After the delay τ, a non-selective $\pi/2$ pulse was employed to detect the longitudinal magnetization.

Affinity indexes were calculated by a linear regression analysis of the NMR parameter values plotted *vs* macromolecule concentration. The fitting of the experimental data was obtained using the program Kaleidagraph 4.0.

2.3. Ketotifen fumarate (KT) characterization

^{1}H NMR (600 MHz, 25 °C, D_2O, pH 7.4) δ (ppm): 2.51–3.41 (8H, $H_{8,8'\text{-}9,9'\text{-}10,10'\text{-}11,11'}$, m), 3.74 (2H, $H_{7,7'}$, s), 6.40 (2H, H_{13}, s), 7.13 (1H, H_2, d, $J_{2,1}$ = 4.9 Hz), 7.21 (3H, $H_{4,5,6}$, m), 7.31 (1H, H_3, m), 7.75 (1H, H_1, d, $J_{1,2}$ = 4.9 Hz).

3. Result and discussion

Selection of NMR methods to investigate drug–macromolecule interactions essentially depends on the need to set a very high ligand to target ratio in order to obtain a detectable NMR signal for the small molecule. On the fast exchange conditions, observed NMR parameter (P_{obs}) is the weighted average of its value for the bound (P_b) and free (P_f) states (Eq. (1), where x_b is the molar ratio of bound drug).

$$P_{obs} = x_b P_b + (1 - x_b) P_f \quad (1)$$

Thus only NMR parameters undergoing a sharp variation as the consequence of macromolecule interaction can be usefully exploited. Chemical shift changes, which are induced by macromolecule binding, are relatively small compared to the line width changes, therefore most NMR studies have been focused on different NMR parameters. Among them, relaxation parameters, and in particular selective relaxation rates (Valensin et al., 1986), are highly sensitive indicators of binding processes between macromolecules and small molecules. In fact, methods based on the determination of selective relaxation rate take advantage of its favorable dependence on the correlation time τ_c in the region of slow molecular motions ($\omega^2\tau_c^2 \gg 1$, where ω is the Larmor frequency), into which the small molecule is forced by the interaction with the macromolecule. In fact, in the fast-motion region ($\omega^2\tau_c^2 \ll 1$), both the selective and non-selective relaxation rates ($R_1{}^{ns}$) increase progressively with increasing τ_c. When the molecular motion of the small molecule is slowed down to the slow-motion region as a consequence of the interaction with the macromolecule, the selective relaxation rate shows a sharp increase, whereas $R_1{}^{ns}$ reaches a maximum for $\omega^2\tau_c^2 \cong 1$ and then it decreases with further increasing $\omega^2\tau_c^2$ (Neuhaus and Williamson, 1989). $R_1{}^{ns}$ is measured by inverting simultaneously all spins and following the recovery of their magnetization during the time. Proton monoselective relaxation rates ($R_1{}^{ms}$) are measured by selective excitation of only one spin, leaving other ones unperturbed. Useful information on the drug–macromolecule interaction can be obtained also by determining the cross-relaxation term σ_{ij} (Valensin et al., 1986; Uccello-Barretta et al., 1991), as the occurrence of ligand–biomacromolecule interaction can be easily verified by comparing the signs of this term in the absence and in the presence of the macromolecule. In fact, molecules belonging to the fast motion region give positive values of σ_{ij}, whereas, in the case of ligands bound to macromolecules, the ligand experiences slow motion conditions and a negative value of σ_{ij} is expected, as shown in Eqs. (2) and (3), respectively, where $\hbar$ is the reduced Planck constant, r_{ij} is the distance between the two protons i and j, and γ is the magnetogyric ratio.

$$\sigma_{ij} = 0.5\gamma^4\hbar^2 r_{ij}{}^{-6}\tau_c \quad (2)$$

$$\sigma_{ij} = -0.1\gamma^4\hbar^2 r_{ij}{}^{-6}\tau_c \quad (3)$$

The cross-relaxation parameters can be determined in a very simple way by measuring the proton mono-($R_1{}^{ms}$) and bi-selective ($R_1{}^{bs}$) relaxation rates (Valensin et al., 1986). Biselective relaxation rates of spin i can be measured by selective excitation of the two spins i and j, leaving other ones unperturbed. The difference between biselective and monoselective relaxation rates gives cross-relaxation terms (Eq. (4)).

$$\sigma_{ij} = R_1{}^{bs} - R_1{}^{ms} \quad (4)$$

A helpful approach to evaluate the strength of interaction between a drug and a macromolecule is the determination of the "affinity index", which is based on linear fitting (Rossi et al., 1997) of experimental data, which are obtained by measuring the NMR parameter (P_{obs}) in solutions containing a constant concentration of drug and variable amounts of the macromolecule. The slope of the straight line of the plot of the NMR parameter (P_{obs}) *vs* the macromolecule concentration gives the "affinity index". This is a function of the association constant (K), the number of binding sites (n), the NMR parameter in the bound state (P_b) and the ligand concentration (C_L) (Rossi et al., 1999) (Eq. (5)).

$$[A] = \frac{KP_b C_L^{n-1}}{1 + KC_L^n} \quad (5)$$

Different sites of the molecule could have different dynamics, leading to effects on the NMR parameters and, as a consequence, on the affinity index values due to different correlation times modulating the dipolar interactions between protons at different positions; the normalization to the NMR parameter in the free state $(P_{obs} - P_f)/P_f$ removes the effect of different correlation times and different proton densities and isolates the effects of restricted motions due to the interaction of the ligand with the macromolecule, leading to obtain the "normalized affinity index" [A^N] (Corbini et al., 2006). The advantage of this parameter is that it provides a measure of drug–macromolecule global affinity which is independent of the stoichiometry of the interaction, and it is

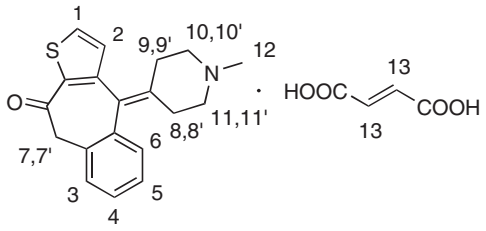

Fig. 1. KT structure.

a powerful tool to compare the interaction strengths of different drug–macromolecule systems.

We measured proton selective relaxation rates of KT (Fig. 1) at 2 mM concentration in D_2O (pH 7.4, phosphate buffer) in the presence of a wide range of BSM concentrations between 0.1 mg/mL and 8 mg/mL. On increasing BSM concentration $R_1{}^{ms}$ values of KT protons underwent a relevant increase, which reflected the contribution to the measured parameter from the mucin-bound KT (Table 1).

High variations were detected with respect to the values measured for KT alone (Table 1), as an evidence of the interaction between the drug and mucin. However, solutions containing macromolecules, as in this case, may be subjected to an increase of viscosity. This phenomenon might cause a slowing down in the dynamics of the ligand and, hence, an increase of relaxation rates, even in the absence of any interaction with the polymer. $R_1{}^{ms}$ of KT fumarate counterion (Fig. 1) was highly diagnostic to this regard. In fact, the observed relaxation parameter of fumarate counterion in absence of BSM was 0.09 s^{-1}, which remained nearly unchanged also in the presence of the highest BSM concentration.

Normalized selective relaxation rate enhancements $(R_{1obs}{}^{ms} - R_{1f}{}^{ms})/R_{1f}{}^{ms}$ (where $R_{1obs}{}^{ms}$ is the selective relaxation rate measured in the mixture, and $R_{1f}{}^{ms}$ is the selective relaxation rate measured for pure drug) were very diagnostic to understand the stereochemistry of interaction, as relaxation rates are local parameters, which depend on the involvement of the different drug sites (and hence nuclei) in the interaction with the macromolecule. In fact, a high variation of their values due to the presence of mucin means a large involvement in the binding processes. Interestingly in the more diluted solution (BSM 0.1 mg/mL) H_3 proton belonging to the condensed phenyl ring showed higher normalized variation of its proton selective relaxation rates, with respect to H_1 proton adjacent to the sulfur nucleus (Table 1). At 0.6 mg/mL of mucin a reversal of the above trend was observed, as H_1 proton showed a slightly higher value (2.27) than that for H_3 proton. On increasing the BSM concentration up to the maximum

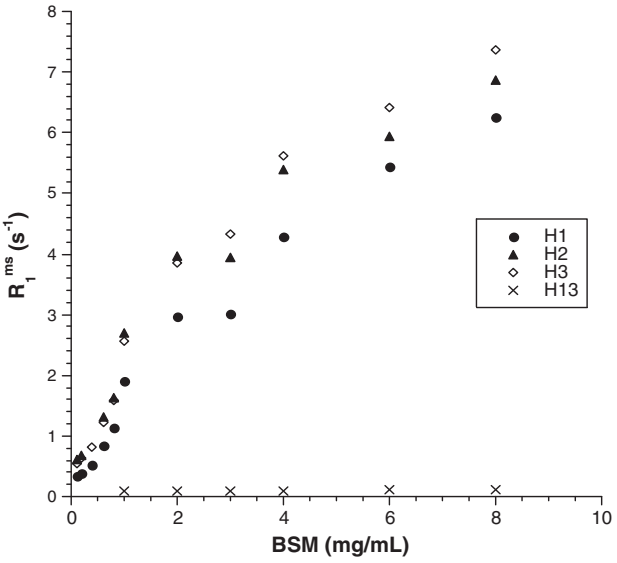

Fig. 2. Dependence of ^1H (600 MHz, 25 °C D_2O, pH 7.4) selective relaxation rates ($R_1{}^{ms}$, s^{-1}) of selected protons of KT (2 mM) on BSM concentration.

value of 8.0 mg/mL the above said values diverged further. The above findings, strongly suggested a change of interaction mode of KT in the two BSM concentration ranges. We can assume proton H_1 as a probe of the interaction of sulfur atom, proton H_3 as a probe of condensed phenyl group interactions, and fumarate counterion H_{13} reflects the degree of involvement of the ring containing the nitrogen atom. Thus, inside the highest range of BSM concentration, the sulfurated moiety seems to be more extensively involved in the interaction with mucin than the condensed phenyl moiety. In the lowest concentration range the opposite is true, as proton H_3 interaction is more favored. In both concentration ranges the saturated ring containing the nitrogen atom should not be significantly involved in the interaction with BSM, as a matter of fact the counterion does not feel the presence of mucin in spite of the fact that, reasonably, it is held in proximity of the nitrogen atom also in the case of not tight ion pairing. In Fig. 2 the dependence of selective relaxation rate of analyzed protons of KT (2 mM, pH 7.4) on the concentration of BSM (from 0.1 mg/mL to 8 mg/mL) is shown. The graph clearly points out that this dependence is not linear, but rather, at about 0.6 mg/mL of BSM, the slope of the line shows a remarkable variation. Thus, in order to evaluate the strength of the interaction of KT–BSM complex, we calculated the affinity indexes from the slopes of the lines describing the dependence of $R_1{}^{ms}$ on BSM concentration inside both of these

Table 1
^1H (600 MHz, D_2O, pH 7.4, phosphate buffer, 25 °C) selective relaxation rates $R_1{}^{ms}$ (s^{-1}) and normalized selective relaxation rates $(R_{1obs}{}^{ms} - R_{1f}{}^{ms})/R_{1f}{}^{ms}$ of selected protons of KT (2 mM) pure and in mixtures with BSM.

[BSM] (mg/mL)	$R_1{}^{ms}$			$(R_{1obs}{}^{ms} - R_{1f}{}^{ms})/R_{1f}{}^{ms}$		
	H_1	H_2	H_3	H_1	H_2	H_3
0	0.26	0.56	0.38	–	–	–
0.1	0.33	0.62	0.56	0.27	0.11	0.47
0.2	0.38	0.69	0.64	0.46	0.23	0.68
0.4	0.53	0.88	0.82	1.04	0.57	1.16
0.6	0.85	1.31	1.21	2.27	1.34	2.18
0.8	1.14	1.64	1.59	3.38	1.94	3.18
1.0	1.91	2.70	2.56	6.35	3.82	5.74
2.0	2.97	3.97	3.85	10.42	6.09	9.13
3.0	3.01	3.94	4.33	10.58	6.04	10.39
4.0	4.29	5.39	5.62	15.50	8.62	13.79
6.0	5.44	5.93	6.41	19.92	9.59	15.87
8.0	6.26	6.88	7.38	23.08	11.29	18.42

Table 2
Affinity indexes ([A], mg^{-1} mL s^{-1}) and normalized affinity indexes ([A^N], mg^{-1} mL) calculated for selected protons of KT (2 mM) with mucin.

Proton	0.1 < [BSM] < 0.8 [A]	1 < [BSM] < 8 [A]	0.1 < [BSM] < 0.8 [A^N]	1 < [BSM] < 8 [A^N]
H_1	1.12	0.62	3.85	2.40
H_2	1.49	0.57	2.67	1.02
H_3	1.49	0.67	3.91	1.75

Table 3
^1H (600 MHz, 25 °C, D_2O, pH 7.4,) selective (R_1^{ms}), bi-selective (R_1^{bs}) relaxation rates of proton pair H_1 and H_2, and calculated cross-relaxation rate (σ_{12}, s^{-1}) of proton pair H_1–H_2 of KT (2 mM) in mixtures with variable amounts of BSM.

[BSM] (mg/mL)	R_1^{ms} (H_1)	R_1^{bs} (H_1)	R_1^{ms} (H_2)	R_1^{bs} (H_2)	σ_{12}[a]
0	0.26	0.31	0.56	0.59	0.04
0.1	0.33	0.34	0.62	0.63	0.01
0.2	0.38	0.36	0.69	0.68	−0.02
0.4	0.53	0.45	0.88	0.86	−0.05
0.6	0.85	0.74	1.31	1.17	−0.12
0.8	1.14	0.91	1.64	1.45	−0.21
1.0	1.91	1.57	2.70	2.34	−0.35
2.0	2.97	2.46	3.97	3.40	−0.54
3.0	3.01	2.43	3.94	3.25	−0.64
4.0	4.29	3.49	5.39	4.40	−0.90
6.0	5.44	4.03	5.93	4.86	−1.24

[a] Calculated as the average value.

ranges of BSM concentration. On the basis of linear fitting of experimental data (Table 1), affinity indexes for the different KT protons were calculated, which are summarized in Table 2. Both the change of mucin–drug affinity in the two concentration ranges and the change of KT interaction stereochemistry are quite difficult to be rationalized. In consideration of the fact that high affinity binding sites are able to originate stronger interactions than low affinity sites do, we would expect an affinity increase in the high concentration range of mucin, whereas the reversal was observed. Therefore, we could hypothesize that changing BSM concentration and, hence, drug–mucin molar ratios, brought about conformational changes of mucin which affected the nature of interaction processes and, therefore, the KT–BSM affinity.

The slowing down of molecular motion of drug as the consequence of the interaction with mucin was efficiently detected by the determination of the cross-relaxation parameters of the proton pair H_1–H_2 in the presence of different concentrations of BSM. Above said parameter, which represents a global parameter of the strength of KT–BSM interaction, was calculated as the difference of the R_1^{bs} and R_1^{ms}, on the basis of Eq. (4). The value of σ_{12} for pure KT (2 mM, pH 7.4) was 0.04 s^{-1} (Table 3), which is in accordance with molecule belonging to fast motion region. σ_{12} progressively diminished its value by increasing mucin concentration as the consequence of the increase of the bound molar fraction. In the presence of 6 mg/mL of mucin, we obtained a value of σ_{12} of −1.24 s^{-1} (Table 3), confirming that the bound molar fraction x_b of KT to BSM was elevated.

Affinity indexes calculated from the straight line obtained by linear regression analysis of cross-relaxation terms *vs* BSM concentration were 0.299 mg^{-1} mL s^{-1} in the diluted range and 0.179 mg^{-1} mL s^{-1} in the concentrated range.

The binding processes between KT and AG were investigated by proton selective relaxation rate measurements in mixtures containing KT (2 mM, D_2O, pH 7.4) and variable amounts of AG, from 2 mg/mL to 50 mg/mL, which was the very high concentration value employed by Burgalassi et al. (2007). We did not detect very high variations of the selected parameters between AG 2 mg/mL and 8 mg/mL (Table 4). Only in correspondence of highly concentrated solutions we obtained detectable variations of NMR parameters. Once again counterion selective relaxation rates underwent negligible variations. Affinity indexes of the system KT–AG, obtained by linear fitting of R_1^{ms} of KT in dependence of AG concentration,

Table 4
^1H (600 MHz, D_2O, pH 7.4, 25 °C) selective relaxation rates R_1^{ms} (s^{-1}) of selected protons of KT (2 mM) in mixtures with AG (variable amounts).

[AG] (mg/mL)	H_1	H_2	H_3
2	0.25	0.52	0.47
4	0.25	0.53	0.49
6	0.26	0.54	0.51
8	0.29	0.58	0.57
20	0.66	1.09	1.11
50	1.19	1.73	1.82

Table 5
Affinity indexes ([A], g^{-1} mL s^{-1}) calculated for selected protons of KT (2 mM) with AG or TSP.

Proton	[A] (AG)	[A] (TSP)
H_1	20.8	48.6
H_2	26.7	79.8
H_3	29.4	101.8

are listed in Table 5. By contrast, as previously reported (Uccello-Barretta et al., 2008), KT showed a good affinity towards TSP, almost two- or threefold superior with respect to AG (Table 5).

Progressively increasing amounts of TSP or AG (between 1 mg/mL and 8 mg/mL) were added to KT/BSM mixtures. KT concentration was fixed at the value of 2 mM which was employed in the analyses all of binary mixtures and a high value of mucin concentration of 4 mg/mL or 3.2 mg/mL was selected, which caused very large perturbations of KT without giving significant viscosity increase.

Addition of TSP to KT–BSM mixtures produced progressively larger variations of proton selective relaxation rates. In particular, we observed a progressive decrease (Fig. 3) of relaxation parameters of KT protons, to confirm that affinity of KT towards mucin diminished as the consequence of the presence of the polysaccharide (Table 6). R_1^{ms} of fumarate proton H_{13} did not change over the whole concentration range.

Then, we analyzed the effect of the other polysaccharide AG on the R_1^{ms} of KT in KT/BSM mixtures. The concentration of the polysaccharide was varied from 0.13 mg/mL to 8 mg/mL. In the entire range of AG concentrations no significant variations of KT relaxation rates were observed (Table 7).

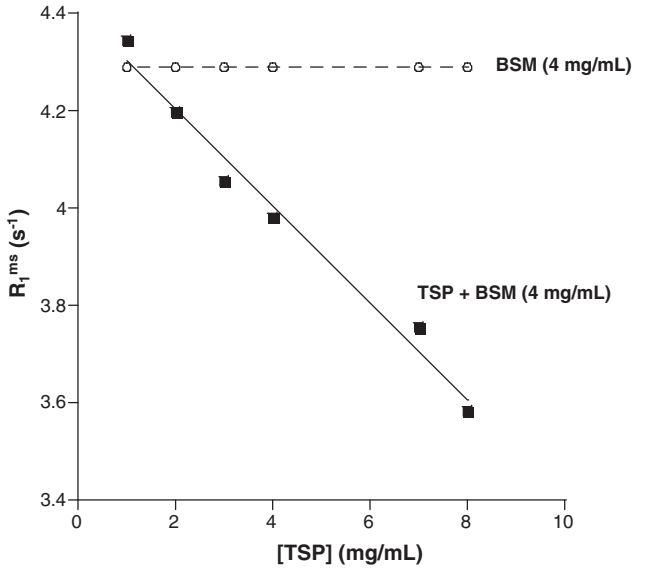

Fig. 3. Plot of selective relaxation rate (R_1^{ms}, s^{-1}) of proton H_1 of KT on TSP concentration. The concentration of KT and BSM are kept constant (2 mM and 4 mg/mL, respectively).

Table 6
Selective relaxation rates R_1^{ms} (s^{-1}) of selected protons of KT (2 mM) in the presence of BSM (4 mg/mL) and different concentrations of TSP.

[TSP] (mg/mL)	H_1	H_2	H_3
0	4.29	5.39	5.62
1	4.34	5.26	5.47
2	4.20	5.04	4.80
3	4.06	5.21	5.28
4	3.98	4.68	4.84
7	3.76	4.70	4.51
8	3.58	4.48	4.74

Table 7
Selective relaxation rates (s^{-1}) of selected protons of KT (2 mM) in the presence of mucin (3.2 mg/mL) and different concentrations of AG.

[AG] (mg/mL)	H_1	H_2	H_3
0.13	3.44	4.27	4.98
0.25	3.33	4.44	4.72
0.5	3.54	4.26	4.82
1.0	3.44	4.22	4.89
8.0	3.46	4.25	4.67

Furthermore, we found that solutions containing AG, BSM and KT were not stable, as in time there was formation of a precipitate and the selective relaxation rates of KT protons in the ternary mixtures KT/BSM/AG underwent progressive decrements after samples preparation. Relaxation parameters of KT remained unchanged in time in the ternary mixtures containing TSP.

4. Conclusions

NMR spectroscopy confirmed (Uccello-Barretta et al., 2010) to be a very useful alternative technique to compare mucoadhesive properties of polysaccharides, by using suitable low-molecular weight probes of their interaction with mucin.

Accordingly to previously reported results (Di Colo et al., 2009) obtained by using rheological method, the large decreases of proton selective relaxation rates of KT in the KT/BSM mixture, in buffered solutions, due to the presence of TSP pointed out mucoadhesive properties of TSP, as the polysaccharide was able to form stable adducts with mucin, thus displacing KT from it. AG polysaccharide, inside the same range of concentrations, did not seem to originate any significant interaction with mucin as it is not able to affect KT/BSM interaction at all. In this way TSP–mucin affinity was found to be remarkably higher than that of AG.

Above findings pointed out the relevance of proton selective relaxation rate measurements for the non invasive a priori evaluation of drug–polysaccharides or polysaccharide to mucin affinities, which open promising prospective in the rational design of new formulation for pharmaceutical uses.

Acknowledgments

This work was supported by MIUR (FIRB Project RBPR05NWWC) and by Farmigea S.p.A.

References

Burgalassi, S., Nicosia, N., Monti, D., Falcone, G., Boldrini, E., Chetoni, P., 2007. Larch arabinogalactan for dry eye protection and treatment of corneal lesions: investigation in rabbits. J. Ocul. Pharmacol. Ther. 23, 541–549.
Chandrasekaran, R., Janaswamy, S., 2002. Morphology of Western larch arabinogalactan. Carbohydr. Res. 337, 2211–2222.
Ch'ng, H.S., Park, K., Kelly, P., Robinson, J.R., 1985. Bioadhesive polymers as platforms for oral controlled drug delivery. 2. Synthesis and evaluation of some swelling, water-insoluble bioadhesive polymers. J. Pharm. Sci. 74, 399–406.
Corbini, G., Martini, S., Bonechi, C., Casolaro, M., Corti, P., Rossi, C., 2006. Synthetic polymers as biomacromolecular models for studying ligand–protein interactions: a nuclear spin relaxation approach. J. Pharm. Biomed. Anal. 40, 113–121.
Di Colo, G., Zambito, Y., Zaino, C., Sansò, M., 2009. Selected polysaccharides at comparison for their mucoadhesiveness and effect on precorneal residence of different drugs in the rabbit model. Drug Dev. Ind. Pharm. 35, 941–949.
Edsman, K., Hägerström, H., 2005. Pharmaceutical applications of mucoadhesion for the non-oral routes. J. Pharm. Pharmacol. 57, 3–22.
Freeman, R., Wittekoek, S., 1969. Selective determination of relaxation times in high resolution NMR. J. Magn. Reson. 1, 238–276.
Ghelardi, E., Tavanti, A., Celandroni, F., Lupetti, A., Blandizzi, C., Boldrini, E., Campa, M., Senesi, S., 2000. Effect of a novel mucoadhesive polysaccharide obtained from tamarind seeds on the intraocular penetration of gentamicin and ofloxacin in rabbits. J. Antimicrob. Chemother. 46, 831–834.
Griffiths, P.C., Occhipinti, P., Morris, C., Heenan, R.K., King, S.M., Gumbleton, M., 2010. PGSE-NMR and SANS studies of the interaction of model polymer therapeutics with mucin. Biomacromolecules 11, 120–125.
Hägerström, H., Edsman, K., 2003. Limitations of the rheological mucoadhesion method: the effect of the choice of conditions and the rheological synergism parameter. Eur. J. Pharm. Sci. 18, 349–357.
Hägerström, H., Stromme, M., Edsaman, K., 2005. Drug molecules as probes for studying the compatibility between gels and mucous tissue with dielectric spectroscopy. J. Pharm. Sci. 94, 1090–1100.
Hassan, E.E., Gallo, J.M., 1990. A simple rheological method for the in vitro assessment of mucin–polymer bioadhesive bond strength. Pharm. Res. 7, 491–495.
Mortazavi, S.A., 1995. An in vitro assessment of mucus/mucoadhesive interactions. Int. J. Pharm. 124, 173–182.
Neuhaus, D., Williamson, M., 1989. The Nuclear Overhauser Effect in Structural and Conformational Analysis. VCH Publisher, New York.
Patel, M.M., Smart, J.D., Nevell, T.G., Ewen, R.J., Eaton, P.J., Tsibouklis, J., 2003. Mucin/poly(acrylic acid) interactions: a spectroscopic investigation of mucoadhesion. Biomacromolecules 4, 1184–1190.
Ponchel, G., Touchard, F., Duchene, D., Peppas, N.A., 1987. Bioadhesive analysis of controlled-release systems. I. Fracture and interpenetration analysis in poly(acrylic acid)-containing systems. J. Control. Release 5, 129–141.
Ponder, G.R., 1998. Arabinogalactan from Western larch. Part IV. Polymeric products of partial acid hydrolysis. Carbohydr. Polym. 36, 1–14.
Rolando, M., Valente, C., 2007. Establishing the tolerability and performance of tamarind seed polysaccharide (TSP) in treating dry eye syndrome: results of a clinical study. BMC Ophtalmol. 7, 5–13.
Rossi, C., Donati, A., Bonechi, C., Corbini, G., Rappuoli, R., Dreassi, E., Corti, P., 1997. Nuclear relaxation studies in ligand–macromolecule affinity index determinations. Chem. Phys. Lett. 264, 205–209.
Rossi, C., Bastianoni, S., Bonechi, C., Corbini, G., Corti, P., Donati, A., 1999. Ligand–protein recognition studies as determined by nuclear relaxation analysis. Chem. Phys. Lett. 310, 495–500.
Smart, J.D., Kellaway, I.W., Worthington, H.E.C., 1984. An in-vitro investigation of mucosa-adhesive materials for use in controlled drug delivery. J. Pharm. Pharmacol. 36, 295–299.
Uccello-Barretta, G., Bertucci, C., Domenici, E., Salvadori, P., 1991. Conformational and dynamic changes of D- and L-tryptophan due to stereoselective interac-

tion with human serum albumin, as revealed by proton-selective relaxation rate measurements. J. Am. Chem. Soc. 113, 7017–7019.
Uccello-Barretta, G., Nazzi, S., Balzano, F., Di Colo, G., Zambito, Y., Zaino, C., Sansò, M., Salvadori, E., Benvenuti, M., 2008. Enhanced affinity of ketotifen toward tamarind seed polysaccharide in comparison with hydroxyethylcellulose and hyaluronic acid: a nuclear magnetic resonance investigation. Bioorg. Med. Chem. 16, 7371–7376.
Uccello-Barretta, G., Nazzi, S., Zambito, Y., Di Colo, G., Balzano, F., Sansò, M., 2010. Synergistic interaction between TS-polysaccharide and hyaluronic acid: implications in the formulation of eye drops. Int. J. Pharm. 395, 122–131.
Valensin, G., Sabatini, G., Tiezzi, E., 1986. In: Niccolai, N., Valensin, G. (Eds.), Advanced Magnetic Resonance Techniques in Systems of High Molecular Complexity. Birkhauser, Boston, pp. 69–76.